A Software Simulation Program for a Hybrid Fuel Cell – Battery Power Supply for an Electric Forklift

Edward Chan*, Francis Dawson*, Henk Bekker**, and Eugene Livshits**
* EDWARD S. ROGERS SR. DEPARTMENT OF
ELECTRICAL AND COMPUTER ENGINEERING, UNIVERSITY OF TORONTO
10 King's College Road
Toronto, Ontario, Canada M5S 3G4
Tel.: 1-416-978-2613
E-Mail: ed.chan.a@utoronto.ca, dawson@ele.utoronto.ca
** Saft Power Systems, 2680 Fourteenth Avenue, Units 1 & 2,
Markham, Ontario, Canada L3R 5B2

Acknowledgements

The authors of this paper would like to acknowledge the support of Saft Power Systems, the Natural Sciences and Engineering Research Council (NSERC) of Canada, the Province of Ontario's Graduate Scholarship program, and the University of Toronto.

Keywords

Fuel cell system, Hybrid power integration, Simulation, Battery charger, Hybrid electric vehicle (HEV)

Abstract

This paper presents the development of a software simulation program for an electric forklift powered by a hybrid fuel cell – battery power supply. The power supply is based on a range extender active hybrid configuration, where a proton exchange membrane (PEM) fuel cell is used to continuously charge a flooded lead-acid battery on-board the forklift. The program involved modelling the discharging and charging characteristics of a flooded lead-acid battery along with the fuel consumption of the PEM fuel cell and the power consumed by the fuel cell's balance of plant components.

Introduction

A forklift is a motorized vehicle that is used for lifting heavy objects. Forklifts are used in a variety of places from factories and warehouses to military bases. Battery powered electric forklifts are the only type of forklift that has regulatory permission to operate indoors or within an enclosed environment. This is because battery powered forklifts do not generate any poisonous exhaust gases unlike the forklifts powered by internal combustion engines [1].

However, there are two main problems with battery powered forklifts. The first problem is that the battery must be recharged after use with externally installed charging equipment that is connected to the grid. Furthermore the recharging event is a time consuming process which reduces the productivity of the forklift [1, 2]. Using traditional charging methods, it takes at least eight hours to fully recharge a forklift battery [2]. Hence these forklifts are limited to areas where charging equipment is installed. The second problem arises from the fact that the forklift's operating time between recharging events depends on the capacity of the installed battery. Typically the battery is designed to provide power for eight hours of operation on a single charge; the length of a typical shift at a factory [2]. However, a problem would

arise if the forklift needed to be used occasionally beyond the designed capacity of the battery, i.e. over-time operation.

Fuel cell technology, specifically Proton Exchange Membrane (PEM) fuel cell technology can be exploited to overcome the problems associated with current battery powered electric forklifts. The problem of lengthy recharging times and limited operation times would be eliminated if fuel cell technology were to replace the battery in electric forklifts, as a fuel cell forklift could be recharged in minutes by adding more hydrogen fuel. Furthermore the use of fuel cells would also remove the necessity of installing expensive on-site external charging equipment. Unfortunately fuel cells are currently unable to supplant the battery in electric forklifts because (1) operating the fuel cell with transient output power demands and repetitive start-up and shut-down cycles reduces the lifespan of the PEM fuel cell [3], (2) the fuel cell cannot react quickly and precisely to changes in electrical load demands due to the slow nature of the fuel cell chemical reactions [4], and (3) fuel cells currently cost much more than equivalent batteries that can provide the same amount of power since fuel cells are not yet mass manufactured [5].

One potential solution that is currently used to eliminate the start-up and transient operation problems with fuel cells is to use the fuel cell as part of a hybrid power source. In such a power supply, the fuel cell is combined with an energy storage device such as a battery or an ultra-capacitor. The focus of this paper is on an electric forklift powered by a hybrid power supply consisting of a fuel cell combined with a flooded lead-acid battery. By using the fuel cell within a hybrid power supply, the problems of start-up and transient operation of the fuel cell are solved by always operating the fuel cell with constant output power and having the energy storage device take care of all transient and start-up demands. The benefits of a hybrid power electric forklift over existing electric forklift technology include:

- Eliminating the recharging time problem of traditional electric forklifts by having the fuel cell recharge the battery on-board the forklift
- Removing the need and expense for external charging and battery swapping equipment
- Increasing worker productivity, as no more time is wasted recharging and swapping batteries as is necessary for traditional electric forklifts
- Allowing for over-time operation

It is important to note that there are currently several companies that are actively researching and developing a hybrid fuel cell electric forklift [6 - 8], however very little information is available in the public domain. Thus, the objective of this paper is to fill the void in publicly available information by examining the power electronics required to connect the battery and fuel cell together and also to explore the operation of the hybrid power source through the development of a MATLAB software simulation program. The program simulates the behaviour of a hybrid powered forklift as it operates through a full day of activities based on steady state models of the battery, fuel cell, and forklift loading characteristics.

The first step in the development of the simulation program for a hybrid powered electric forklift is to decide on how to connect the battery and the fuel cell together and also to decide on the relative sizing of the two power supplies. The hybrid power supply must satisfy the following requirements:

- Power needs to be supplied to the load instantaneously on demand
- The hybrid configuration must be able to recharge the battery whenever the forklift is idle
- The output voltage of the power supply should be the same as the batteries currently used in electric forklifts in order to minimize conversion costs
- The fuel cell needs to operate with constant power output or equivalently constant current output to maximize its lifespan
- Current cannot be allowed to flow into the fuel cell. Cell reversal may occur with consequent damage to the fuel cell if current flows into the fuel cell [9]

Hybrid Power Supply Configurations

Passive and Active Hybrid

The methods that can be used to link the fuel cell and battery together to form a hybrid power supply can be broadly classified into two categories: passive hybrids and active hybrids [10]. In a passive hybrid, the fuel cell and the battery are connected directly together to the load [10]. The advantage of this method is its simplicity and low cost. The main disadvantage of this method is that it provides the user with no control over the power flow between the fuel cell and the battery. The power flow between the two power sources is instead dictated by the internal impedance of each source [10]. As a result, it is not possible to ensure that the fuel cell operates with constant current output which is a design requirement for the forklift hybrid power supply. In contrast, control over the fuel cell output current is possible with the use of an active hybrid.

In an active hybrid, the fuel cell and the battery are connected to the load via a Multiple Input Power Electronic Converter (MIPEC) [10, 11]. A MIPEC consists of at least one DC / DC converter along with a DC link and / or a transformer [12]. The DC / DC converter allows for the control of the output current from the fuel cell, and thus allows for the control of the fuel cell output power which is a design requirement for the hybrid powered forklift. Thus the active hybrid configuration was the one selected for the hybrid powered electric forklift. The power conversion topology that was selected for the hybrid power supply is shown in Fig. 1. As shown in Fig. 1, the fuel cell is connected to the battery and the forklift via a current controlled boost DC / DC converter. The input and output voltages of the boost converter are fixed by the fuel cell output voltage (V_{FC}) and the battery output voltage (V_{bat}) respectively. When the forklift is active, power to the forklift is supplied by both the battery and fuel cell. When the forklift is idle, power from the fuel cell is used to recharge the battery.

The selection of a boost DC / DC converter automatically prevents current from flowing into the fuel cell either from the battery or from load regeneration due to the presence of a diode in the topology. Also with this converter topology, the battery is directly connected to the forklift. Therefore all of the forklift's instantaneous power demands can be met by the battery, like in a traditional electric forklift. As a result, this design automatically meets another design requirement, that the output voltage of the power supply should be the same as the batteries currently used in electric forklifts in order to minimize conversion costs. The main disadvantage of this topology is that it cannot control load regeneration current flow into the battery. A solution to this problem would be to place an additional resistor in parallel with the battery to act as a current sink for any excess current that the battery could not absorb. This would be a lower cost solution than to increase the number of DC / DC converters in the MIPEC to allow for the control of the regenerative load current.

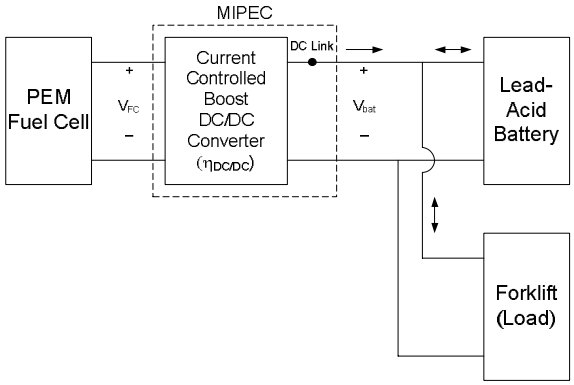

Fig. 1: Hybrid Power Supply Converter Topology

 ISBN : 9789075815108

Sizing of the Fuel Cell and the Battery

The next step is to select the relative sizing of the battery and the fuel cell. Depending on the relative sizes of the output power of the fuel cell and the capacity of the battery, a fuel cell – battery hybrid power supply can either be classified as a power assist hybrid, a medium hybrid, or a range extender hybrid as summarized in Fig. 2 [13].

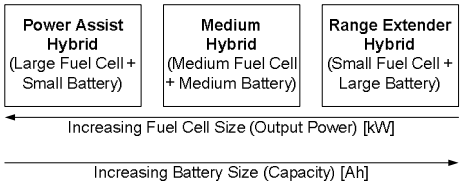

Fig. 2: Hybrid Classification

The range extender hybrid configuration was selected for the hybrid powered electric forklift mainly for economic reasons since it uses a relatively small fuel cell compared to the other two hybrid types. Generally the larger the fuel cell, the more expensive it will be [13]. Using a larger battery is not an important factor as currently batteries are less expensive than fuel cells; approximately ten to twenty times less expensive [5]. In a range extender hybrid, the battery provides all average and peak power demands from the load while the fuel cell is only responsible for recharging the battery. The next step is to model the two power sources. It is important to note that a full model of the battery and fuel cell are beyond the scope of this paper and only characteristics that are pertinent to the simulation program are detailed.

The Flooded Lead-Acid Battery

The main characteristic of the flooded lead-acid battery that needs to be modelled for the software simulation program is the battery's depth of discharge (DoD(t)). The depth of discharge as shown in (1) is the fraction of the battery capacity that has been withdrawn from the battery at a given time. The depth of discharge value of the battery in the hybrid power supply is continuously changing: increasing as the battery supplies charge to power the forklift and also decreasing as the battery is recharged either by the fuel cell or by load regeneration. It is important to note that the depth of discharge is limited to 0.80 (the discharge limit) for the lead-acid battery in order to prevent deep discharge. Deep discharging reduces the life span of the battery [14, 15].

$$DoD(t) = \frac{Q_{Withdrawn}(t)}{Q_P(t)} \tag{1}$$

where $Q_{Withdrawn}(t)$ is the amount of charge withdrawn from the battery at time t and $Q_p(t)$ is the battery capacity at time t.

Another important property of a battery is the battery's percent state of charge (%SoC). The %SoC of a battery is the percentage of its capacity remaining at a given time. The relationship between the %SoC and the DoD of a battery is shown in (2).

$$\%SoC(t) = (1 - DoD(t)) \times 100\% \tag{2}$$

In the simulation program, one method is used for calculating changes in the DoD(t) of the battery during discharge events and another method is used during charging events. Aging, temperature, and self-discharge effects of the battery are neglected.

 ISBN : 9789075815108

Discharge Mode

The discharge current of the battery in the hybrid power supply continuously varies as the forklift moves and lifts loads. Thus a dynamic model for the battery's DoD was used for the simulation program. The fractional depletion model, as shown in (3), is based on Peukert's equation and was used to model the dynamics. The fractional depletion model tracks the change in the DoD of the battery ($\Delta DoD_{Discharge\ Event}$) over a period of time Δt.

$$\Delta DoD_{\text{Discharge Event}}(\Delta t) = \frac{I_{\text{discharge}}^{n}}{K}\Delta t \tag{3}$$

where n is the Peukert number for the battery, K is a fitting parameter, and $I_{discharge}$ is the discharge current. The complete derivation of the model can be found in [14].

Charge Mode

The charging of a flooded lead-acid battery proceeds in two phases, Phase 1 and Phase 2 depending on value of the battery's state of charge, as illustrated in Fig. 3. If the battery is charged when its %SoC is less than a value ε, then Phase 1 charging occurs otherwise Phase 2 charging occurs. For a flooded lead-acid battery, ε ranges from 75 to 80 % [16]. Very few losses occur during Phase 1 charging and as a result in this paper this charging phase is assumed to be lossless [15]. Thus during Phase 1 the charge supplied to the battery ($Q_{supplied,Phase1}$) is equal to the charge stored by the battery ($Q_{stored,Phase1}$). On the other hand during Phase 2, not all of the charge provided to the battery is stored. Instead some of the charge is used to split water stored inside the battery into oxygen and hydrogen gas; this reaction is also known as electrode gassing [15]. The charge used for electrode gassing is considered to be a loss. As a result during Phase 2, the charge supplied to the battery ($Q_{supplied,Phase2}$) is greater than the charge stored by the battery ($Q_{stored,Phase2}$).

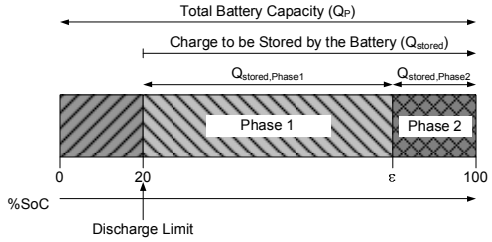

Fig. 3: The Two Phases of Charging for a Lead-Acid Battery

Phase 1 Charging

If during Phase 1 the battery is supplied with a charging current ($i_{charge}(t)$) starting at time t_1 and ending at time t, then the amount of charge stored by the battery ($Q_{stored,Phase1}(t)$) can be determined using the relationship shown in (4).

$$Q_{\text{supplied,Phase1}}(t) = Q_{\text{stored,Phase1}}(t) = \int_{t_1}^{t} i_{\text{charge}}(\tau)d\tau \tag{4}$$

As the battery is charged, the battery's depth of discharge decreases as charge is stored by the battery. By offsetting the amount of charge previously withdrawn from the battery at the beginning of the charging process with the charge stored during the charging process, the depth of discharge of the battery can be determined by combining (1) and (4) together, as shown in (5). For a small time period over which the charging current is constant (I_{charge}), the change in the battery's depth of discharge (ΔDoD_{Phase1}) over this time period ($\Delta t = t - t_1$) can be simplified to the relationship shown in (6).

 ISBN : 9789075815108

$$DoD(t)_{\text{Phase1}} = \frac{Q_{Withdrawn}(t_1) - \int_{t_1}^{t} i_{\text{charge}}(\tau)d\tau}{Q_P(t_1)} \quad (5)$$

$$\Delta DoD_{\text{Phase1}}(\Delta t) = \frac{-I_{\text{charge}}\Delta t}{Q_P(t_1)} = -I_{\text{charge}}\Delta t \frac{DoD(t_1)}{Q_{Withdrawn}(t_1)} \quad (6)$$

Phase 2 Charging

As described previously, in Phase 2 some of the charge provided to the battery is stored while some of it is used for electrode gassing; the charge used for electrode gassing is deemed as a loss. The amount of charge used for gassing and the amount of charge actually stored by the battery must be determined before the model for Phase 2 can be developed. Generally, the charging losses for batteries are stated for the entire charging period and are not broken down into the losses for Phase 1 and Phase 2. The losses are described by the battery charging factor or charge coefficient (α). The charge factor as shown in (7) gives the ratio between charge supplied to ($Q_{supplied}$) and charge that is stored (Q_{stored}) by the battery for a complete charging event, i.e. the battery is charged starting with a %SoC of 20% and ending with the %SoC at 100% as shown in Figure 3 [15]. Since there are losses during the charging process, the value for α is always greater than one. For a lead-acid battery, α ranges from 1.1 to 1.2 [17]. In order to account for the two charging phases, the relationship for α is also shown in its expanded form in (7).

$$\alpha = \frac{Q_{\text{supplied}}}{Q_{\text{stored}}} = \frac{Q_{\text{supplied,Phase1}} + Q_{\text{supplied,Phase2}}}{Q_{\text{stored}}} \quad (7)$$

The charge factor for each charging phase is also defined as shown in (8) and (9).

$$\alpha_{\text{Phase1}} = \frac{Q_{\text{supplied,Phase1}}}{Q_{\text{stored,Phase1}}} \quad (8)$$

where α_{Phase1} is the charge factor during Phase 1 charging

$$\alpha_{\text{Phase 2}} = \frac{Q_{\text{supplied,Phase2}}}{Q_{\text{stored,Phase2}}} \quad (9)$$

where α_{Phase2} is the charge factor during Phase 2 charging

However as previously discussed, the first charging phase is lossless, i.e. the charge supplied is equal to the charge stored by the battery. As a result, the charging factor for the first phase (α_{Phase1}) is equal to 1. Thus, along with the use of Fig. 3 and (7), the relationship shown in (9) can be simplified as shown in (10).

$$\alpha_{\text{Phase2}} = \frac{0.8}{(1-\varepsilon)}(\alpha - \frac{(\varepsilon - 0.2)}{0.8}) \quad (10)$$

If Phase 2 starts at time t_2 and ends at time t, then by using the reasoning provided previously for the lossless charging phase, the depth of discharge during the second charging phase can be determined using the relationship shown in (11). For a small time period over which the charging current is constant (I_{charge}), the change in the battery's depth of discharge (ΔDoD_{Phase2}) over this time period ($\Delta t = t - t_2$) can be simplified to the relationship shown in (12).

 ISBN : 9789075815108

$$DoD(t)_{\text{Phase2}} = \frac{Q_{Withdrawn}(t_2) - \int_{t_2}^{t} \frac{i_{\text{charge}}(\tau)}{\alpha_{\text{Phase2}}} d\tau}{Q_P(t_2)} \tag{11}$$

$$\Delta DoD(\Delta t)_{\text{Phase2}} = \frac{-\frac{I_{\text{charge}}}{\alpha_{\text{Phase2}}}\Delta t}{Q_P(t_2)} = -\frac{I_{\text{charge}}}{\alpha_{\text{Phase2}}}\Delta t \frac{DoD(t_2)}{Q_{Withdrawn}(t_2)} \tag{12}$$

The PEM Fuel Cell

The role of the PEM fuel cell in the hybrid power supply is to continuously recharge the battery. This allows the fuel cell to operate with a constant output power (P_{FC}). The program models the rate of fuel consumption of the fuel cell and the net fuel cell output power. For simplification, the simulation program does not model any start-up or shut-down transients.

Fuel Consumption Rates

The amount of hydrogen fuel consumed by the fuel cell can be calculated using (13) [18]. At the rate shown in (13), the amount of air needed to support the fuel cell chemical reaction is shown by (14) [18].

$$\text{H}_2 \text{ flow rate} = \frac{P_{FC}}{2F\mu_F V_{cell}} \qquad [mol/s] \tag{13}$$

where F is the Faraday constant (96 489 C), μ_F is the fuel utilization coefficient, and V_{cell} is the mean voltage of each of the individual fuel cells within a fuel cell stack [V] [18]. V_{cell} can range from 0.6 to 0.7 V and a common estimate for V_{cell} is 0.65 V while a common value for μ_F is 0.95 [18].

$$\text{Air flow rate} = \dot{m}_{air} = \frac{(28.964\times10^{-3})\lambda P_{FC}}{0.84FV_{cell}} \qquad [kg/\text{sec}] \tag{14}$$

where λ is the factor by which the air flow rate should be greater than the stoichiometric rate so that all cells in a fuel cell module receive sufficient oxygen [18]. A common value for λ is 2 [18].

Balance of Plant Components

For PEM fuel cells, there is a difference between the gross output power (P_{FC}), the power that the fuel cell module produces from its chemical reactions and the net fuel cell output power ($P_{FC,Net}$), the actual amount of power available for use. This difference arises because some of the gross output power is consumed internally in the fuel cell by its balance of plant (P_{BOP}) components that are necessary to support the operation of the fuel cell. Balance of plant components include an air compressor to compress the input air to the operating pressure of the fuel cell, an ejector to decompress the input hydrogen fuel to the operating pressure of the fuel cell, and a cooling system for the fuel cell. The remaining power that is available to the user is referred to as the net fuel cell output power ($P_{FC,net}$) as shown in (15).

$$P_{FC,Net} = P_{FC} - P_{BOP} \tag{15}$$

The electrical power consumed by the cooling system ($P_{CoolingSystem}$) can be calculated using (16). The power consumed by the air compressor ($P_{compressor,electrical}$) can be calculated using (17). The definitions and common values for the parameters in (16) and (17) are summarized in Table I [18]. The ejector which

 ISBN : 9789075815108

is used to lower the pressure of the stored hydrogen gas does not require any electrical energy. The total power consumed by the balance of plant components can be calculated using (18) and is usually less 30% of the gross fuel cell output power. The software simulation program is discussed next.

$$P_{Cooling\ System} = \frac{P_{FC}\left(\frac{1.25}{V_{cell}} - 1\right)}{SCE} \tag{16}$$

$$P_{compressor,electrical} = \dot{m}_{air} C_p \frac{T_1}{\eta_m \eta_c}\left(\left(\frac{p_2}{p_1}\right)^{\frac{\gamma-1}{\gamma}} - 1\right) \tag{17}$$

Table I: Fuel Cell Balance of Plant Definitions and Common Values

Parameter	Definition	Common Value
C_p	The specific heat of air at a constant pressure	1004 J/(kg·K)
T_1	The temperature of the environment surrounding the fuel cell	293.15 K
p_1	The pressure of the environment surrounding the fuel cell (Atmospheric Pressure)	101.3 kPa
p_2	The operating pressure of the fuel cell	> 200 kPa
γ	The ratio of the specific heat of air at a constant pressure and the specific heat of air at a constant volume (C_v) ($\gamma = C_p/C_v$)	1.4
η_c	The isentropic efficiency of the compressor as specified by the manufacturer of the compressor	0.6
η_m	The mechanical efficiency of the compressor as specified by the manufacturer of the compressor	0.98
SCE	System Cooling Effectiveness [18]	20

$$P_{BOP} = P_{compressor,electrical} + P_{Cooling\ System} \tag{18}$$

The Software Simulation Program

The simulation program tracks the behaviour of the battery and fuel cell by monitoring various performance metrics of the hybrid powered forklift as it operates through a full day of activities. The components that were modelled in the simulation program are summarized in Fig. 4.

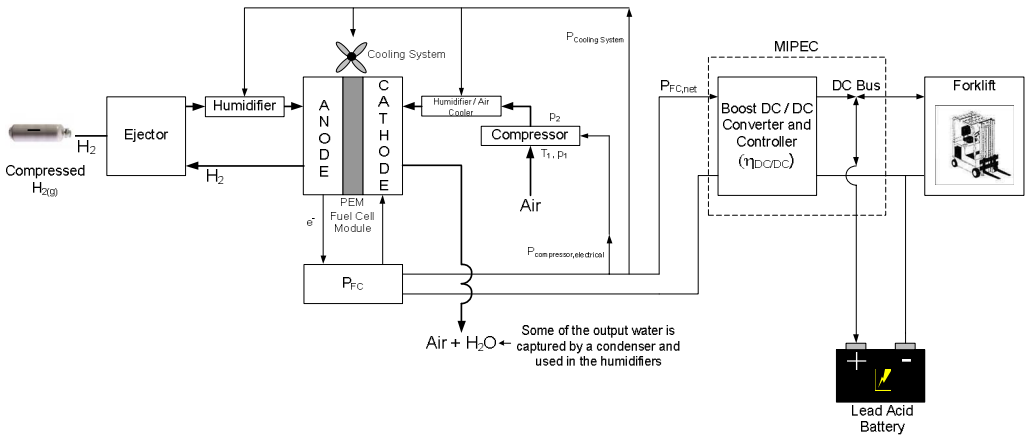

Fig. 4: Elements Modeled in the Simulation Program

The program was developed by linking the models of the fuel cell and battery in a range extender – active hybrid configuration. The performance metrics that are monitored include the battery state of charge (%SoC) and the amount of fuel consumed by the fuel cell.

The software simulation program for the hybrid powered forklift was developed using the longitudinal dynamics simulation method and was implemented using MATLAB [19]. In the program, the behaviour of the forklift during the day is described by a continuous series of discrete time intervals. Within each interval, a percentage of the time is assigned to each of the following forklift actions: lifting a load, moving at constant speed, idling, braking, and lowering a load. The length of the interval period is inversely proportional to the accuracy of the simulation, i.e. the smaller the interval period, the higher the accuracy [19]. The performance metrics or characteristics of the forklift are calculated at the end of each interval period. For simplification, variable speed operation of the forklift was not included in the simulation program. In the program it is assumed that the transition from one forklift action to another occurs instantaneously. An example of the output from the simulation program is shown in Fig. 5 using component values shown in Table II for a forklift operated over eight hours ($T_{workday}$) where it spends 5% of the time lifting loads, 5% of the time lowering loads, 18% of the time moving laterally, 5% of the time braking, and 67% of the time idling. For the remainder of the day ($T_{overnight}$), the forklift is idle.

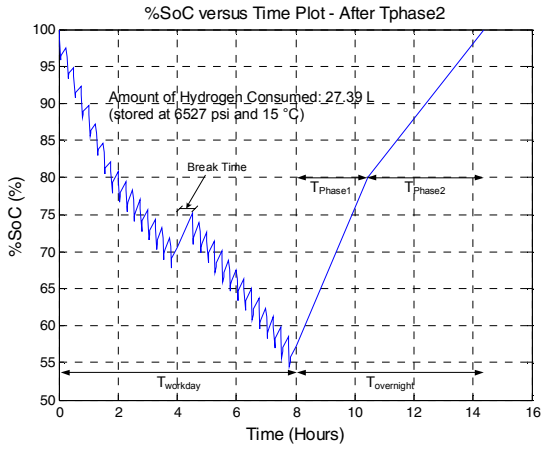

Fig. 5: %SoC versus Time Plot Based on the Values Shown in Table II

Table II: Values used in Simulation Program

	Characteristic	Value
Forklift (Load Currents for Lifting, Moving Laterally at a Constant Speed, Braking, and Lowering)	$I_{lifting}$	183.30 A
	$I_{constant\ speed}$	137.50 A
	$I_{braking}$	-68.75 A
	$I_{lowering}$	-91.65 A
Flooded Lead – Acid Battery	V_{bat}	48 V
	K	480 Ah
	n	1.2
	α	1.2
	ε	80 %
PEM Fuel Cell	P_{FC}	1.2 kW
	I_{FC}	46 A
	V_{FC}	26 V
	p_2	200 kPa
	SCE	20
Boost DC / DC Converter	$\eta_{DC/DC}$	0.8

 ISBN : 9789075815108

One can observe from Fig. 5, the effect of the gassing losses which reduces the charge transferred to the battery during charging events whenever the battery's %SoC is greater than 80%. Also, the net fuel cell output power ($P_{FC,Net}$) was calculated by the program to be 999.51 W, thus approximately 17% was lost to the balance of plant components of the fuel cell.

Conclusion

This paper summarized the development of a software simulation program designed specifically to track the performance of the battery and fuel cell in a hybrid powered electric forklift. The results of the simulation program can then be used to adjust the size of the battery and fuel cell so that they meet the requirements for the range extender hybrid configuration while minimizing the size and cost of the battery and fuel cell. Future work would include validating the models used in the simulation program with physical measurements.

References

[1] W. König, "Battery-Powered Traction – The User's Point of View," in *Battery Technology Handbook*, 2nd ed., H.A. Kiehne, Ed. New York: Marcel Dekker, Inc., 2003, pp. 155-185.

[2] Aerovironment Inc., "Fast Charging Electric Lift Trucks and Industrial Vehicles," [Online], [cited 2005 Aug 18], Available: http://www.aerovironment.com/area-ipc/gen2425.pdf

[3] R. Borup, J. Davey, D. Wood, F. Garzon, and M. Inbody, "DOE Hydrogen Program, PEM Fuel Cell Durability, FY 2005 Progress Report," [Online document], [cited 2006 Aug 31], Available: http://www.hydorgen.energy.gov/pdfs/progress05/vii_i_3_borup.pdf

[4] G. Sauer and O. Carlisle, "The Alkaline Fuel Cell in Mobile Applications," in *Fuel Cells for Automotive Applications*, R. H. Thring, Ed. New York: ASME Press, 2004, pp. 15-29.

[5] J. Loring, "Out of the Shadows," *Report on Business*, vol. 22, No. 9, pp.45-54, April 2006.

[6] Hydrogenics Corporation, "Fuel Cell Powered Forklift", Data Sheet, 2004.

[7] "FIAMM, Nuvera to Develop Hybrid Battery / Fuel Cell Forklift Power," *Fuel Cells Bulletin*, vol. 7, p. 4, 2003.

[8] General Hydrogen, "Class 1 Hydricity Pack," [Online document], [cited 2006 Aug 21], Available: http://www.generalhydrogen.com/hydricity_class1.shtml

[9] K. Rajashekara, "Propulsion System Strategies for Fuel Cell Vehicles," in *Fuel Cell Technology for Vehicles*, R. Stobart, Ed. Warrendale, PA: Society of Automotive Engineers, Inc., 2001, pp. 179-187.

[10] L. Gao, Z. Jiang, and R. A. Dougal, "Evaluation of Active Hybrid Fuel Cell / Battery Power Sources," *IEEE Tran. Aerospace and Electronic Systems*, vol. 41, pp. 346-355, Jan. 2005.

[11] L. Solero, A. Lidozzi, and J. A. Pomilio, "Design of a Multiple-Input Power Converter for Hybrid Vehicles," *IEEE Tran. Power Electronics*, vol. 20, pp. 1007-1016, Sep. 2005.

[12] H. Tao, A. Kotsopoulos, J. L. Duarte, and M. A. M. Hendrix, "Multi-Input Bidirectional DC-DC Converter Combining DC-Link and Magnetic-Coupling for Fuel Cell Systems," presented at the IEEE Industry Applications Conference Fortieth IAS Annual Meeting, Kowloon, Hong Kong, China, 2005.

[13] D. J. Friedman, T. Lipman, A. Eggert, S. Ramaswamy, and K. H. Hauer, "Hybridization: Cost and Efficiency Comparisons for PEM Fuel Cell Vehicles," presented at the 2000 SAE Future Transportation Technology Conference, Costa Mesa, California, United States of America, 2000.

[14] I. Husain, *Electric and Hybrid Vehicles: Design Fundamentals*, Boca Raton: CRC Press, 2003.

[15] H. Bode, *Lead-Acid Batteries*, New York: John Wiley and Sons Inc., 1977.

[16] T. R. Crompton, *Battery Reference Book,* 2nd ed., Oxford: Butterworth-Heinemann Ltd, 1995.

[17] E. Wehrle, "Charging Methods and Techniques: General Requirements and Selection of Chargers," in *Battery Technology Handbook*, 2nd ed., H.A. Kiehne, Ed. New York: Marcel Dekker, Inc., 2003, pp. 291-315.

[18] J. Larminie and A. Dicks, *Fuel Cell Systems Explained*, 2nd ed. Chichester: John Wiley and Sons Ltd., 2003.

[19] J. Van Mierlo and G. Maggetto, "Innovative Iteration Algorithm for a Vehicle Simulation Program," *IEEE Transactions on Vehicular Technology*, vol. 53, pp. 401-412, Mar. 2004.